Room Temperature Superconductivity: the Roles of Theory and Materials Design

Warren E. Pickett
Department of Physics and Astronomy, University of California Davis, Davis, California 95616
(Dated: April 13, 2022)

For half a century after the discovery of superconductivity, materials exploration for better superconductors proceeded without knowledge of the underlying mechanism. The 1957 BCS theory cleared that up: the superconducting state occurs due to pairing of electrons over the Fermi surface. Over the following half century higher critical temperature T_c was achieved only serendipitously as new materials were synthesized. Meanwhile the formal theory of phonon-coupled superconductivity at the material-dependent level became highly developed: given a known compound, its value of T_c, the superconducting gap function, and several other properties of the superconducting state became available independent of further experimental input. More recently, density functional theory based computational materials design has progressed to a predictive level – new materials can be predicted on the basis of various numerical algorithms. Taken together, these capabilities enable theoretical prediction of new superconductors. Here the process that resulted in three new highest temperature superconductors, predicted numerically, confirmed experimentally – SH_3, LaH_{10}, and YH_9 – is recounted. These hydrides have T_c in the 200-280K range at megabar pressures, and here the development will be chronicled. Current activities and challenges are discussed, together with Regularities in compressed hydrides that can guide further exploration.

I. PROLOGUE

Room temperature superconductivity (RTS) has been one of the grand challenges of condensed matter physics since the BCS theory of pairing (see Sec. II) was proposed and its predictions verified. The remarkable electronic and magnetic properties of the superconducting state readily suggests revolutionary applications, both in the laboratory and in industry. The slow progress in increase in the critical temperature T_c from 4K in 1911 to 23K in 1973 – 3K/decade – followed by a 15 year plateau, moved this grand challenge well into the background. The discovery of high T_c cuprates (up to 125K, or 165K under pressure), involving magnetic interactions, introduced a new type of superconductivity (SC) and generated renewed excitement. After eight years of advancement of T_c, another plateau in cuprate superconducting T_c has lasted for (so far) 25 years.

Much attention has centered on guidelines ('rules,' or 'roadmaps') necessary for higher T_c, thereby presumably pointing the way to higher T_c. Such rules have always been based on known superconductors, and have subsequently been set aside as entirely new classes of superconductors were discovered, almost entirely by serendipity. In the 1960s empirical trends led to "Matthias's Rules." These stated that for high T_c one should search for (1) cubic materials, (2) d electrons, and (3) specific electron/atom ratios. This latter rule was soon understood to mean a high density of electron states at the Fermi level ε_F N(0), *i.e.* a high density of superconducting carriers. Bernd Matthias's group had been the leader in the discovery of new superconductors in the 1950s and early 1960s, after which the search extended worldwide.

Though unwritten, additional rules were advertised: (4) stay away from oxygen, which produces unpredictable behavior including insulation, and (5) stay away from magnetism, which at the time competed too strongly with superconducting pairing. Matthias had an additional personal rule: (6) stay away from theorists, they are no help. (Matthias did write[1], without elaboration "I never realized how many of my friends are theorists.") This last rule was based on his observation that knowing the theory of SC, at least in a broad model BCS way, had been useless in helping discovery; what worked (but ploddingly so) was just to "follow the simple roadmap." However, the rules did not produce high T_c materials. It continued to be true through cuprate days – after the initial high T_c – that theory played no part in the advance of the maximum T_c from 30K to 125K in cuprates.

However, over the decades theory and applications advanced. While overt activity toward higher BCS superconductivity waned, intellectual interest in the goal of RTS survived, with evidence given by various international workshops indicating continued interest in room temperature explorations.[2] With the discovery of extreme high T_c SC in compressed metal hydrides under pressure discussed in this paper, the roles of experiment and theory evolved; theory has assumed a prominent role as predictor beyond the maximum known T_c (T_c^{max}) for phonon-coupled SCs as they jumped from 40K to 200K, then rapidly marched toward room temperature.

After recounting the sequence of necessary theoretical advances in Sec. II, Sec. III gives an indication of the computational implementations that were required for application to real materials. An overview of the rising research area in this century of crystal structure prediction is given in Sec. IV. Section V provides a concise description of the revolutionary discoveries of critical temperatures in the 200-260K range. So far these all require megabar pressures. The discussion in Sec. VI gives an impression of near-term challenges and opportunities in the RTS arena, and several regularities of high

T_c compresses hydrides that may guide the next level of searches are listed in Sec. VII. Section VII provides a brief Epilogue.

II. THEORETICAL DEVELOPMENTS THROUGH THE DECADES

The impetus for this stunning breakthrough has been a sequence of advances in theory and computational design together with mastery of high pressure techniques. Since this advance in theory has extended over six decades (*i.e.* 2-3 generations of physicists), we provide in this section an overview of the fertile path of theoretical breakthroughs that have enabled current capabilities and their paradigm-revising results.

A. BCS Theory

In 1957 Bardeen, Cooper, and Schrieffer published their 30-page *magnus opus* "Theory of Superconductivity."[3] This theory introduced a correlated manybody wavefunction based on Fermi surface pairing of electrons demonstrated a year earlier by Cooper. This wavefunction described a thermodynamic condensate of correlated pairs below a critical temperature T_c, assuming an attractive effective pairing potential arising from exchange of phonons and screened electron-electron scattering. The primary result of their theory was the T_c equation (units $\hbar$=1, $k_B = 1$)

$$T_c^{BCS} = 1.14\ \Omega\ e^{-1/\lambda^*} \tag{1}$$

where Ω is the characteristic phonon frequency. $\lambda^* = N(0)V$, where the Fermi level density of states $N(0)$ is a measure of the density of electrons interacting through the phenomenological coupling V, which BCS noted is the net interaction of phonon attraction plus Coulomb repulsion: $\lambda^* = \lambda - \mu^*$ in terms of terminology developed later (see below), λ is the measure of the attractive pair coupling strength by exchange of phonons. Out of interest for the following content of this article we note that the strong coupling limit $\lambda^* \to \infty$ leads in this expression to a maximum SC temperature of 1.14 Ω, which can be well above room temperature. The theory is however only valid for weak coupling, leaving open the question of high T_c. "High T_c" would only be confronted three decades later with the discovery of cuprate superconductors, which are paired by a different mechanism, and hereafter not considered.

The second property of note, provided by BCS theory, is the superconducting gap $[\Delta(\omega, T)]$ equation that gives T_c when linearized ($\Delta \to 0$) and provides the frequency ω and temperature T dependence of the energy gap that is responsible for many of the fascinating properties of superconductors: the fact that a perfect "superconductor" can have a gap for excitations; this gap leads to a vanishing magnetic susceptibility in its interior; it is a basic player in zero resistivity; it severely alters thermodynamic, optical, and transport properties. The effect on the electronic specific heat, shown in Fig. 1, is to make it vanish exponentially as T→0. The theory was soon generalized by Gor'kov, using thermodynamic field theory, to derive[4] the much used 1950 phenomenological free energy theory of Ginzburg and Landau.[5] This extension of theory also provided a direction for pursuing necessary developments, especially a microscopic understanding of total electron-electron interactions in metals, a path that is discussed in subsections below.

B. Migdal-Eliashberg Theory

The microscopic Migdal+Eliashberg (ME) theory (1960) of electron-phonon (EP) coupled superconductivity, weak or strong, followed very quickly after the model BCS theory (1957) based on a model pairing Hamiltonian and a variational treatment. Recall that the full, exact (non-relativistic) Hamiltonian $\mathcal{H}$ for a system of ions $\{\vec{R}\}$ and electrons $\{\vec{r}\}$ is given by

$$\begin{aligned} \mathcal{H} &= [\mathcal{T}^{el}(\{\vec{r}\}) + \mathcal{V}^{el-el}(\{\vec{r}\})] \\ &+ \mathcal{V}^{el-ion}(\{\vec{r}\},\{\vec{R}\}) \\ &+ \mathcal{T}^{ion}(\{\vec{R}\}) + \mathcal{V}^{ion-ion}(\{\vec{R}\}) \end{aligned} \tag{2}$$

in terms of the various kinetic $\mathcal{T}$ and potential $\mathcal{V}$ energies. The middle term contains the (bare) electron-ion interaction. With roughly 10^{20} dynamical coordinates per mm^3, this all-encompassing operator is the fundamental, intractable feature of materials theory that requires innovative approaches and approximations.

Migdal formalized the observation[6] that the great differences in energy scales (or velocities, or masses) of electrons and ions leads to negligible contributions beyond second order perturbation theory in EP scattering. Eliashberg made the formidable step of placing the theory within the newly developed many-body theory (thermal Green's function) that made it applicable to the superconducting state,[7,8] leaving generalizations to materials with crystal structure and lattice effects as a later step (see below). This ME formalism provided the fundamental equations for calculating the gap function (superconducting order parameter), given the Eliashberg spectral function $\alpha^2F(\omega)$ defined in Sec. III.B that provides the essential input for the pairing process. Calculation of this function necessitated several theoretical and algorithmic advances.

C. Density Functional Theory (DFT)

Hohenberg, Kohn, and Sham followed immediately (1965-1967) with density functional theory,[9,10] which makes the full crystalline Hamiltonian in Eq. 3 treatable for many properties of materials for electrons in

their ground state, given a reasonable approximation for many body effects (through an exchange and correlation functional). (The many following extensions of DFT to other properties are not relevant here.) An extremely important aspect of DFT is that it provides a highly reliable one-electron ('mean field') set of band energies and wavefunctions[10] for use in themselves, and also for applications in treating dynamic behavior that is averaged over in DFT. This DFT breakthrough accelerated activity in band theory, already in progress since the late 1930s, based on more phenomenological grounds. The late 1970s saw the accomplishment of achieving self-consistent electronic charge densities, bands, and wavefunctions. Many applications of (electronic) ground state energies were explored in the 1980s and following.

Calculation of energies for any configuration of atoms enabled the evaluation of interatomic force constants between displaced atoms, and thereby phonon spectra. Initially this was accomplished for each phonon independently, but capabilities were rapidly extended, especially by applying density functional perturbation theory (allowing higher order to be obtained analytically) and Wannier function techniques.[25–27] The outcome was true harmonic phonon frequencies through formalism making use of infinitesimal atomic displacements. The change in the electronic potential due to an atomic displacement is the root factor in EP coupling, and calculation of EP matrix elements was achieved only around 2000. Though it has not been instrumental in the topic discussed here, for interest we mention that density functional theory for superconductors (SCDFT) by Gross's group was nearing implementation by 2005.[11]

D. Extension of ME Theory to Real Materials

Also in the mid-1960s, the challenge of addressing real superconductors versus simplified models, a prerequisite for materials design and discovery, was accomplished by Scalapino *et al.* in 1964.[12,13] Starting from the full Hamiltonian of a solid (Eq. 3) they derived a remarkably complete formalism for the superconducting Green's function and the full frequency dependence of the complex gap function. Their formalism awaited a viable description of the underlying electronic energy bands and phonon frequencies, and their coupling. The DFT capabilities discussed in Sec. II.C would provide the underlying electronic bands and wavefunctions, phonon dispersion curves and polarizations, and EP matrix elements.

The validity of their formalism, which underlies today's numerical implementation, relies on a few approximations. One is Migdal's theorem mentioned above: the vast differences in masses of electrons and ions (more precisely, differences in the frequencies of their dynamic responses) specifies that second order perturbation theory is sufficient for the electron and phonon self-energies. Secondly, electron-electron Coulomb repulsion effects leave the metal as a conventional Fermi liquid, specifically, the possibility of magnetic order and magnetic fluctuations is not included at the level we discuss here. Thirdly, the symmetry that is broken at the superconducting phase transition is so-called gauge symmetry; in picturesque language, two electrons can form a Cooper pair and disappear into the condensate, or the inverse process can happen. Finally, for EP-coupled superconductors it is nearly always the case that the superconducting order parameter is proportional to the gap function, *i.e.* a complex scalar and not a vector or tensor quantity, and other symmetries are not broken at T_c. The resulting theory has passed numerous tests as being accurate for EP-coupled superconductors.

E. Analysis of T_c; discussion of a maximum

McMillan in 1968 provided a seminal analysis[14] of T_c and its dependence on $\alpha^2F(\omega)$, presenting his iconic "McMillan equation" expressing T_c via two materials quantities, the phonon frequency θ and λ. A phenomenological retarded Coulomb repulsion μ^* was included in the Eliashberg equation that was solved to relate T_c to α^2F. The results for various α^2F functions were fit to a generalization of the BCS equation of the form

$$\begin{aligned} T_c^{McM} &= \frac{\theta}{1.45} exp\left[-1.04\frac{1+\lambda}{\lambda-\mu^*-0.62\lambda\mu^*}\right] \\ &\equiv \frac{\theta}{1.45} exp\left(-\frac{1+\lambda}{\lambda-\mu^*_{eff}}\right)^{1.04} \end{aligned} \quad (3)$$

where the second expression emphasizes the generalization of the BCS relation. The constants provided best fits to the computational data. The "effective Coulomb repulsion" $\mu^*_{eff} = \mu^*(1+0.62\lambda)$ reflects how strong coupling can be interpreted as enhancing the Coulomb repulsion, and the $1+\lambda$ factor in the numerator is the strong-coupling effect of electron mass renormalization by EP coupling. The mass enhancement is well known to increase the density of active states at the Fermi level, but in this expression the effect in the numerator is to decrease T_c, compensated by the effect of the denominator. Flores-Livas *et al.* have reproduced the model that gives this analytic result, for $\mu^*(\lambda=0)$ and a different expression for the prefactor.[75] In McMillan's time the experimental Debye frequency θ was the most accessible measure of the frequency spectrum, however McMillan recognized that using values from α^2F (such as the second moment ω_2) would be more representative.

Only values of λ<1 were included in McMillan's fit; extrapolation of T_c^{McM} shows that it saturates for large λ; the equation is accurate only for moderately strongly coupled superconductors. The limited range of input was missed or forgotten by many readers, and until the discoveries discussed in the next section one could still find statements in the literature and in presentations that "theory shows that the maximum T_c is limited, perhaps to around 40 K." This point will be clarified shortly.

In 1973 Bergmann and Rainer (BR) noted:[15] to increase T_c, we need to understand the effect on T_c due to an added increment of coupling $\Delta\alpha^2F(\omega)$ at frequency ω. It seemed clear from the BCS equation that adding coupling at high frequency, seemingly increasing both ω (or Ω, or θ, depending on viewpoint) and λ, would raise T_c.

The definitions of λ and the second frequency moment are

$$\lambda = 2\int d\omega \frac{\alpha^2F(\omega)}{\omega}, \quad (4)$$

$$\omega_2^2 = \frac{2}{\lambda}\int d\omega\omega^2 \frac{\alpha^2F(\omega)}{\omega}. \quad (5)$$

Aside from normalization, they are different moments of $\alpha^2F(\omega)/\omega$. The expression for α^2F is given and discussed later.

From α^2F, McMillan had obtained the relation for elemental metals that connected these two descriptors

$$\lambda = \frac{N(0)I^2}{M\omega_2^2} \equiv \frac{\eta}{\kappa}, \quad (6)$$

The numerator $\eta = N(0)I^2$ is the McMillan-Hopfield factor that reflects an "electronic stiffness," where I^2 is the square of the electron-displaced ion scattering matrix element, and the average is over the Fermi surface. The denominator $\kappa = M\omega_2^2$ is the standard harmonic oscillator form of lattice stiffness (force constant). All are normal state properties. This relation indicates that increasing ω_2, which helps T_c, will decrease λ, hurting T_c. However, the T_c equation (any of them) prominently involves a frequency prefactor, indicating a strong tendency for an increased frequency scale to increase T_c. Study by Allen soon after McMillan[16,17] gave suggestions that, due to this complex interdependence of materials properties, including $N(0)$ and I^2, coupling at low frequency might even be harmful for T_c. We return to this issue for compressed hydrides later.

BR addressed the question, in its simplest form, by calculating the differential quantity in the kernel of

$$\Delta T_c = \int d\omega \frac{\delta T_c[\alpha^2F,\mu^*]}{\delta\alpha^2F(\omega)}\Delta\alpha^2F(\omega) \quad (7)$$

They established that this functional derivative is always non-negative (thus every phonon helps, at the BR level). At least for conventional shapes and strengths of α^2F it has a broad peak around $\omega \sim 2\pi T_c$ followed by a slow decrease at high frequency, shown in Fig. 1(c). That result, viz. that coupling at high frequencies is most important, does not quite resolve all issues. While adding some differential coupling $\Delta\alpha^2F(\omega)$ does affect both λ and ω calculated from α^2F, within the larger picture it also will affect the EP coupling that causes changes in α^2F at frequencies besides ω. This effect is not included by simply including a single (extrinsic) increment in α^2F.

Building on the work of McMillan, Allen and Dynes (AD) in 1975 presented a re-analysis[18] of T_c, using more than two hundred solutions to the Eliashberg equation for λ up to 10 and μ^* up to 0.20, and experimental determinations of α^2F (by numerical inversions of tunneling data) with associated measured T_c. AD chose to generalize the McMillan equation. Most obvious is that the frequency prefactor from ω_2 (altered earlier from McMillan's θ) to the logarithmic moment ω_{log} with an adjusted constant, as the latter produced a better fit to their data.

More importantly, they observed that corrections were needed for both the strength of coupling – they considered much larger values of λ – and for the shape of the α^2F/α spectrum. For example, the textbook shape of the Nb phonon spectrum is much different from that of (say) PhD, which consists of low frequency Pd acoustic modes separated from high frequency H optic modes. We return to the implications of this two-peak shape in Sec. VI.B.

The shape dependence was framed by AD in terms of ω_2 in comparison to ω_{log}, the logarithmic frequency moment. IN their fit to extensive data, the argument of the exponent was not changed, rather each change (strong coupling and shape) was incorporated into its own prefactor f_1 and f_2 respectively. The AD equation can be written, considering the McMillan form given above,

$$T_c^{AD} = \frac{\omega_{log}}{1.20}\frac{1.45}{\theta}f_1(\lambda,\mu^*)f_2(\omega_{log},\omega_2)T_c^{McM}(\lambda,\mu^*)$$
$$. = \frac{\omega_{log}}{1.20}f_1f_2exp\left[-1.04\frac{1+\lambda}{\lambda-\mu^*-0.62\lambda\mu^*}\right]. \quad (8)$$

The expressions for f_1 and f_2 can be found in the original paper.[18] Note that θ cancels in the first expression, and is replaced by the logarithmic frequency moment, which AD found to be the most useful moment for the prefactor of T_c. Note that due to the f_1 and f_2 factors, T_c^{AD} is not exponential in λ except where λ begins to approach μ^* (very weak coupling) where it is highly sensitive to each quantity, nor is it a meaningful fit to any data. For the high T_c compressed hydrides discussed in Sec. V, each prefactor can approach a 10-20% enhancement of T_c (or increasingly more as λ is increased still further).

A crucial finding of AD was that in the large λ regime, where analytic results could be extracted,

$$T_c \to 0.15\sqrt{\lambda\omega_2^2} = 0.15\omega_2\sqrt{\lambda} = 0.15\sqrt{\eta/M} \quad (9)$$

for $\mu^* = 0.10$ (the prefactor depends somewhat on μ^*). Here $\lambda = \eta/(M\omega_2^2)$ for elements has been used to display different viewpoints. A primary results is that Eliashberg theory poses *no limit on* T_c. Figure 1(d) shows some of the numerical data that establishes the rising (not plateauing) of $T_c(\lambda)$, and panel (e) provides numerical data using experimental shapes of α^2F.

Another informative observation is that, as far as the limiting value goes, neither λ nor ω_2 are separately relevant; physically, increasing λ decreases ω_2 and there are numerous examples of this. It should be recognized that performing this limit assumes nothing else happens except that λ increases. This procedure is non-physical;

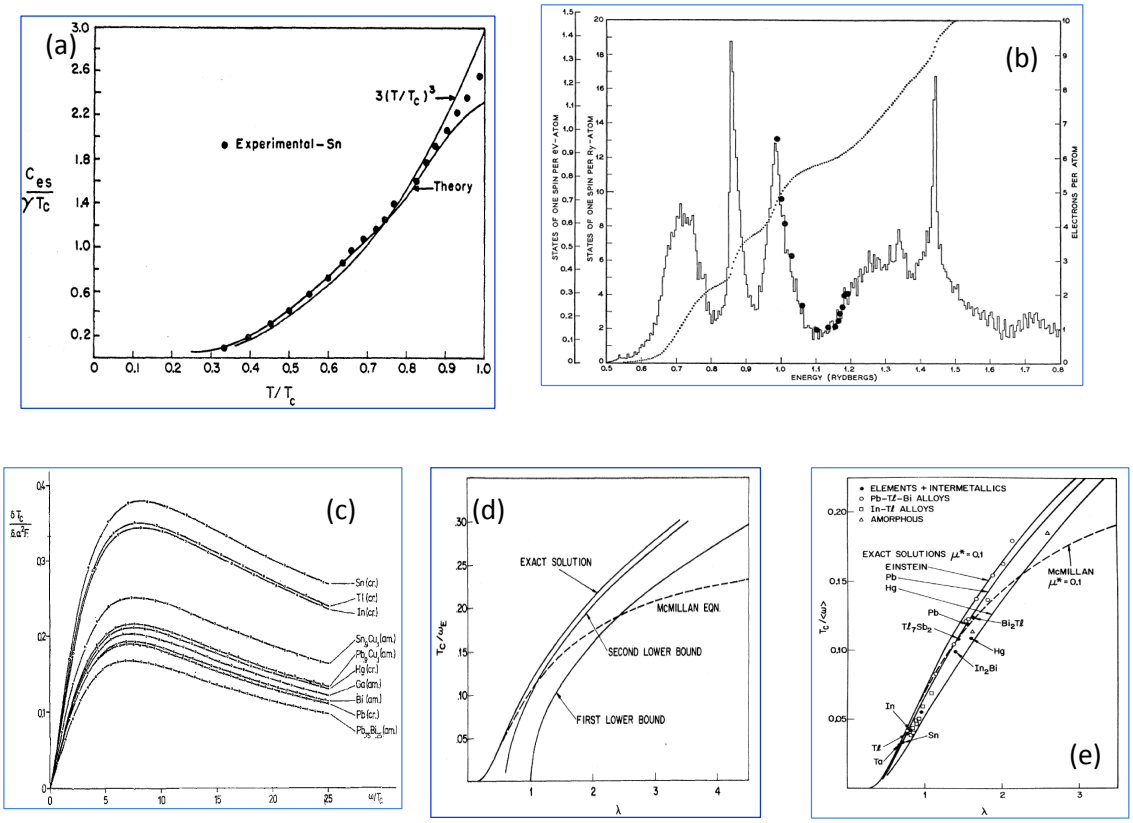

FIG. 1: Numerical data from important early papers that extended theoretical understanding of T_c. (a) Figure from the BCS (1957) paper illustrating the predicted temperature dependence of the specific heat in the superconducting state to the normal state value (equal to 1.0 on the abscissa). The behavior is exponentially small at low temperature. (b) McMillan's plot, for $5d$ transition metal alloys, of the experimental values of (dots) the band structure Fermi level densities of states, for which the mass enhancement $1+\lambda$ of the specific hear γ has been removed, compared to the band theory calculation of tungsten by L. F. Matthiess. The agreement is remarkable. (c) Bergmann and Rainer's plots of $\delta T_c/\delta\alpha^2F(\omega$ versus frequency ω for a number of superconductors (as labeled). Its value peaks near $\omega = 2\pi T_c$ and decreases slowly thereafter, indicating little importance of low energy phonons, great importance for higher energies. (d) Allen and Dynes' (1975) plots the ratio $T_c/ < \omega >$ versus λ for the McMillan equation, and for truncated and exact numerical results from the Eliashberg equation. (e) Similar plots (from Allen and Dynes (1975)) using data for several known strong coupled superconductors. Also shown is the exact solution for an Einstein model with frequency $< \omega >$, and the deviation from the McMillan equation beginning at $\lambda \sim 1$. Here $< \omega >$ is the conventional first moment of α^2F.

making changes that increase λ in turn decrease frequencies due to the increased coupling from electronic states at higher energy. Increasing λ often creates lattice instabilities, so the more strongly coupled material cannot exist. Still, nothing prohibits finding superconductors with increasingly larger λ and higher T_c. Further analysis of T_c can be found in extended descriptions by Allen[19,20] and Allen and Mitrović.[21]

III. APPLYING THE THEORY

With the DFT-ME theory in hand, the periodic table and compilations of known superconductors provided an imposing number of possible applications: which materials systems are the most interesting for study. This question is discussed briefly in this section, with the question of how to sample the many possibilities is described in the following section.

A. Choice of the Favorable Materials Platforms

Regarding ever higher T_c, transition metal based materials had been sampled and studied, experimentally and theoretically, by 2010, and promising directions were few. Considering possibilities more generally, the favored palette of atomic constituents for higher, possibly room temperature, superconductors, had already been presented in two suggestions by Ashcroft. In 1968, while research focused on transition metal compounds, he proposed elemental metallic hydrogen as a very high T_c material,[22] based on (1) its small mass favoring high frequencies, and (2) the vibrating proton, which if not too strongly screened should provide the strong scattering that would be required for pairing at high frequencies. These properties were supported by the BCS Eq. 1, since little of a material-specific nature was understood relating to higher T_c. Ashcroft understood that it would require high pressure to metalize hydrogen, specifically to break the H_2 molecular bond to create an "atomic hydrogen metal" and bring strong scattering processes to the Fermi energy. That it would require 500 GPa (five megabar) or more[23] to break the H_2 bond may not have been anticipated.

The theoretical and computational capabilities to address this question would not be available until the next century. Skipping ahead: in 2004 Ashcroft refocused his concept, arguing[24] that hydrogen-rich molecules, viz. CH_4, NH_3, etc., could circumvent the challenge of breaking the strong H_2 bond by replacing it with a weaker bond, and also provide "precompression" in the experiment, thereby lowering the required pressure to produce what would be essentially metallic hydrogen. Section V reveals how remarkably successful this path has been.

B. Computational Implementation

The formalism and some important analysis was complete by the mid-1980s, where self-consistent DFT calculations could provide the electron wavefunctions and band structures giving Fermi surfaces in excellent agreement with experiment, and phonons were becoming available but were still challenging computationally. The expression for the Eliashberg function illustrates one of the computational bottlenecks:

$$\alpha^2F(\omega) = N_\uparrow(0)\frac{\sum_{kk'}|M_{kk'}|^2\delta(\omega-\omega_{k-k'})\delta(\varepsilon_k)\delta(\varepsilon_{k'})}{\sum_{kk'}\delta(\varepsilon_k)\delta(\varepsilon_{k'})} \quad (10)$$

where the Fermi energy ε_F=0, and k-k' is the wavevector of the phonon scattering an electron from state k to k'. Necessary sums over bands and phonon branches are implicit. The sums that are shown are each over the three dimensional Brillouin zone, confined by the pair of δ-functions to lines of intersection of the Fermi surfaces, requiring fine meshes for convergence. For clarity, the density of states factor is for a single spin, designated by the arrow on $N_\uparrow(0)$. The denominator reflects that this expression is the double average of $|M^2|$ over the line of intersection of two Fermi surfaces with relative displacement $Q = k' - k$, all done in ω-resolved fashion.

To emphasize the numerical challenge, we note that the EP matrix element M requires the computation of the self-consistently screened potential due to the phonon displacements, then requiring evaluation of the matrix element between electron states k and k' on the Fermi surface, with necessary band and phonon branch indices. This extensive computation has, through innovative algorithms, been brought to viable although still time-consuming level. The electron states are expressed in terms of localized Wannier functions,[25] and the phonons are expressed in terms of localized lattice Wannier functions.[26,27] This combination considerably speeds the various required zone samplings. The linear response algorithms have been implemented to enable the phonon-induced change in screened potential to be calculated from the formal infinitesimal-displacement limit.

Beyond the basic DFT formalism and codes, evaluating α^2F required a sequence of advancements of formalism and construction of codes, many of which were adapted to parallel computation. In lieu of attempting to describe them, we refer the reader to a modern, extensive review article on the EP formalism with several of the algorithms,[28] and a monograph on materials modeling,[29] by Giustino.

IV. CRYSTAL STRUCTURE PREDICTION

A. General recent activities

The previous section described the developments that led to the current capability: given a dynamically stable specific compound, the EP coupling strength λ, superconducting T_c, and several properties of the superconducting state can be calculated reliably. Design of new superconductors requires a separate capability: the prediction of new crystalline materials. Design and discovery of new materials was an occasional occurrence until the several agency-wide U.S. program *Designing Materials to Revolutionize and Engineer our Future* (DMREF) was initiated in 2011. The idea was to push the ever expanding computational power to design new materials and properties, to accelerate experimental discovery, then to speed time to market of new products. Many new programs have supported this initiative, which emphasized computational theory-experiment partnership and research, development, and industry synergy.

Materials design, even restricting oneself to crystalline materials with modest sized unit cells, is a challenging process. First is the choice of number of elements (we discuss binaries) and their stoichiometry, with some chosen property in mind but initially in the background. A great deal is known about structural phases of elemental materials, and about the concentration-temperature

phase diagrams of several binary compounds, and certain ternary classes at ambient pressure. Given the periodic table of 100 elements (X,Z), there are $\sim$ 5000 X-Z pairs, dozens of stoichiometries, and for each, as many as dozens of reasonable structures. For a brute force search, a DFT relaxation would be required for each, certainly a daunting task. Classification into the 230 space groups can help to organize the exploration, but samples with first order transformations readily skip over space group symmetries.

The focus in this paper is on Ashcroft's suggestion of H-rich materials, which for binaries reduces the search drastically to $X\mathrm{H}_n$ compounds, but leaves a still challenging task (here the formula is normalized to one X atom). The focus here is compressed hydrides, adding the pressure variable to the space to be explored. The challenge is to identify candidates that are metallic and thermodynamically stable (metastable phases that are not far from stability may be of interest), then check whether they are dynamically stable. Finally, calculation of electron bands and wavefunctions, and the phonon spectrum, followed by α^2F. Then calculation of T_c, $\Delta(\omega,T)$, and a few other properties of the superconducting state can be carried out.

To identify thermodynamic stability (compounds that will not decompose into two or more phases with lower energy) for any chosen pressure P and temperature T, an efficient numerical scheme is required due to the computational complexity of the exercise. Fundamentally, the goal is to identify, for a given stoichiometry $X\mathrm{H}_n$, the minimum enthalpy H(P,T) over the possible crystal structures. Somewhat more precisely, one really needs for the most precise prediction the minimum of the Gibbs free energy

$$\begin{aligned} \mathcal{F}(P,T) &= [E(P,T)+PV(P,T)]-TS(P,T) \quad (11) \\ &\equiv H(P,T)-TS(P,T), \end{aligned}$$

in terms of the internal energy E, volume V, and entropy S (mostly lattice vibrational at temperatures of interest). It is found that the lattice zero-point energy in $E(0,0)$, which is more important for hydrogen than for heavier atoms, and the entropy term can shift phase boundaries. The zero point energy and entropy requires calculation of the phonon spectrum, but much screening of candidates can be done without this step. The volume V and internal structural parameters are relaxed (at T=0) to get the enthalpy $H(P,0)$, and the vibrational entropy is calculated when that level of precision is desired. When $H(P,0)$ iv plotted versus concentration the resulting curve is called the convex hull. The minimum gives the predicted most stable stoichiometry, which is calculated for each pressure of interest.

B. Evolutionary prediction

An enabling capability in the structural search has been the development, in this century, of evolutionary crystal structure prediction. There are a few methods in use, but the concept is to choose a few candidate structures, relax them, and compare properties, especially the total energy, or under pressure, the formation enthalpy. The most favorable candidates are chosen to guide the construction of new candidates – typically, derived "evolutionarily" by some algorithm – until the most favorable candidate is obtained (for a given n and a given cell or supercell size, as a practical limitation).

Crystal structure prediction progressed from early random sampling, basin-hopping, and force-field molecular dynamics to first principles DFT-based enthalpy comparisons, often outlining the convex hull of thermodynamic crystal stability. Modern methods, with some prominent ones (with clues to methods contained in their acronyms) being CALYPSO[30] (Crystal structure AnaLYsis by Particle Swarm Optimization), USPEX[31] (Universal Structure Predictor: Evolutionary Xtallography), AIRSS[32] (Ab Initio Random Structure Searching), and XtalOpt[33] (crystal structure prediction and optimization), incorporate various algorithms from simulated annealing, evolutionary/genetic algorithms, minima or basin hopping, particle swarm optimization, metadynamics, and (quasi)random searches,[34] to search the necessarily broad configuration space. A monograph can be consulted for further information.[35]

Actual procedures differ, and the likelihood of finding the true stable formation enthalpy minima is constrained by a few factors, such as unit cell size (faced by all methods) and the effort spent to sample the full phase space, which as mentioned is a daunting task. A typical procedure might proceed as follows. After choices of metal atom, H concentration n, and some candidate structures, the volume and atomic positions are relaxed subject to the chosen pressure. In early steps faster methods with somewhat lower precision can be used. Evolutionary steps based on the most favorable candidates produce new candidate structures. The process is continued (a computationally taxing procedure) until negligible improvement is occurring, signaling convergence. The H concentration n is changed and the process repeated; sometimes this is automated. Varying n, which for a given system can involving hundreds of thousands of structures,[36] the "convex hull" delineating the stable compounds in this binary system can be plotted. Examples of the convex hull of SH_3 at relevant pressures are shown in Fig. 2(a). This method, involving enthalpy calculated from DFT. has proven successful in predicting stable candidates. Various chosen pressures must be computed independently.

Candidate structures then must be checked for dynamic stability (absence of imaginary frequencies indicating unstable displacements) to be valid predictions. Stability can be determined either by phonon spectrum calculations or by *ab initio* molecular dynamics. Only then can the DFT-ME theory be applied to obtain T_c and a selection of other desired properties obtained from the gap equation. The procedure for full search for high

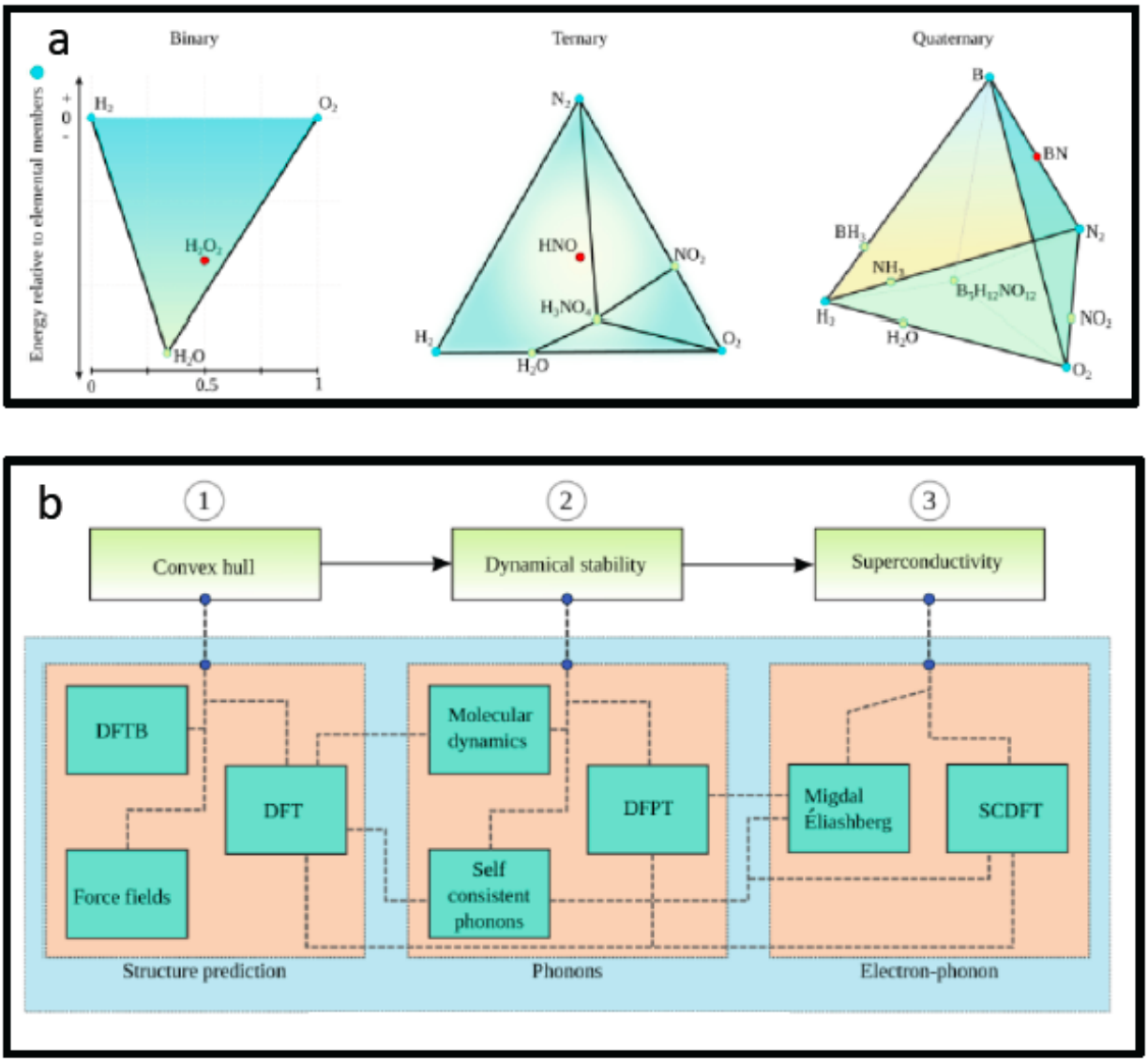

FIG. 2: (a) For the SH_n system, the computed convex hull, with specific calculated formation enthalpies with respect to elemental S and H_2. Shown are pressures of 100, 200, and 300 GPa for the stoichiometries that were obtained in the search. SH_3 is lowest on the convex hull (the straight solid lines) for all three pressures. Convex hulls often have more compounds on or near the hull (more evident convexity of the solid line), and may be obtained from hundreds or thousands of enthalpy calculations. Adapted from Ref. [37] with permission. (b) An example of the progression of the high T_c search program. First, the thermodynamic stability is obtained from compounds on the convex hull. Second, dynamic stability is studied, and phonon spectra are obtained. Third, the DFT-ME calculation: EP coupling and the phonon spectrum to obtain $\alpha^2F(\omega)$, and T_c is obtained from the Eliashberg equation or from one of the fit expressions $T_c(\lambda, \mu^*, \omega_{log}, \omega_2)$. DFTB, DFPT, and SCDFT indicate separate DFT-based capabilities.

T_c is outlined in schematic form in Fig. 2(b). The preferred stable candidate(s) has been identified. Then EP coupling and $\alpha^2F(\omega)$ is calculated (also a big step), after which T_c can be obtained from the Eliashberg theory or established fits to earlier fits to solutions to Eliashberg equations.

C. Machine learning, data mining

As in many of the sciences and elsewhere, machine learning techniques are being applied to materials design, but few yet with applications to compressed hydrides. The basic idea is pattern recognition: provide a large database to give the neural net the opportunity to identify certain characteristics ("training") that are (statistically) related to given descriptors. The procedure

produces likely candidates for the desired characteristics (viz. T_c) with rectitude estimated by various statistical measures. While earlier applied to address other materials properties, applications to general superconducting materials have been implemented. A large database of known superconducting materials exists, consisting of the compound formula, crystal structure, and T_c. However, no experiment-derived database for compressed hydrides exists due to the dearth of examples, so training must be done on to predicted cases.

The machine learning study of hydrides by Hutcheon *et al.* provides an instructive example.[38] For descriptors for candidates MH_n, they chose H content (n), and the metal element (M) size (van der Waals radius), atomic number, mass, and electronic configuration (number of s, p, d, f electrons). Notice that these descriptors have little direct relation to the quantities that determine λ or phonon frequencies or interactions. The result identified the first three columns of the periodic table as best candidates for M, a feature already noted in various overviews. These low electron affinity elements give up much or even all of their valence electrons to the H sublattice. This added charge raises the H $1s$ occupation above the half-filled level, promoting metallicity. In studies of atoms M across the entire periodic table, a few outliers exist: atoms with open d or even f shells. Interestingly, the first discovery, SH_3, is a different sort of outlier, with sulfur's open, roughly half-filled p shell.

V. THE BREAKTHROUGH DISCOVERIES: THEORY THEN EXPERIMENT

A. High pressure experimentation

According to Ashcroft's original concept,[22] metallic atomic hydrogen should provide the acme of T_c, since the atom has the smallest mass, with highest frequencies if force constants are strong, and the potential for strong scattering of electrons by proton displacements seemed likely. Calculations sometimes including the quantum nature of the proton have predicted the stable structures versus pressure. The predictions are T_c of 500K or higher,[23] requiring pressures of 500 GPa or higher. Few attempts have reached a static pressure this high, so Ashcroft's second suggestion[24] has been the avenue of choice: use H-rich molecules as the ambient pressure sample to avoid strong H_2 bonding and antibonding states being pulled away from the Fermi level, and to exploit precompression (higher H concentration and density).

Another point merits mention. Over past decades there have been reports of signals of possible room temperature superconductivity, usually in resistance or susceptibility measurements, which are the most straightforward evidences of superconductivity. The samples are invariably polycrystalline and/or porous, or multiphase, or disordered to the point of amorphous. When such signals are not reproducible, they have made the community skeptical to the point that "USO" is a recognizable acronym – unidentified superconducting object. It is possible that some of them could be evidence of interface superconductivity or some other unusual type, but if not reproducible a report does not receive extended notice.

For this reason the discoveries below focus on reproducible results, noting confirmations. It must however be recognized that the samples in diamond anvil cells are far from the ideal single crystals that are often available at ambient pressure. The compounds are synthesized within the cell as megabar pressures and temperatures up to 2000K are varied. Samples will typically be polycrystalline, strained, and multiphase, and with hard-to-determine stoichiometry. For first order phase transitions the free energy barriers may be high, making it challenging to reach certain Gibbs energy minima. For these reasons various confirmations of these first three discoveries of approaching or near room temperature superconductivity will be noted. Also, given the complexities of samples (mentioned above) at a given P and T, experimental data will not be uniform across groups, nor even across a given lab's runs, so "reproducibility" and comparison with theoretical predictions should be interpreted accordingly.

B. SH_3: the initial breakthrough

Theory. In 2014 Li *et al.*[39] employed the CALYPSO structure prediction code[30] to identify candidate structures with SH_2 stoichiometry at high pressure. Note that this formula is isovalent with H_2O, and the molecules are isostructural. The much more strongly bonded H_2O is known to remain insulating up to the current highest static pressure. Their study, finding insulating structures at lower pressures, focused on a transition between two predicted metallic structures in the 130-160 GPa region. The lower pressure compound has a low symmetry $P\bar{1}$ space group, polymeric structure, with an atomic H $Cmca$ phase with a layering of H and of S atoms occurring at higher pressure. The calculated T_c was maximum at the transition (∼160 GPa), around 60K in the $P\bar{1}$ structure and 82K for $Cmca$, and decreasing with pressure in this latter phase. The maximum coupling strength, occurring at the structural transition, was λ=1.25, with 40% attributed to S modes (which comprise 1/3 of the phonon branches).

Appearing immediately after, also in 2014, was a prediction by Duan *at al.*[40] that for a SH_3 stoichiometry [labeled at the time after the initial constituents, $(H_2S)_2H_2$), and later as H_3S], a high symmetry, atomic H structure was predicted to be the most stable one in the 150-200 GPa range, and the calculated T_c peaked just above 200K in the 160-200 GPa region. Coupling strength λ=2.2 was calculated, with 25% arising from the low energy S modes. The cubic structure has one of the highest symmetries possible for this stoichiometry: SH_6 octahedra are connected by H atoms which

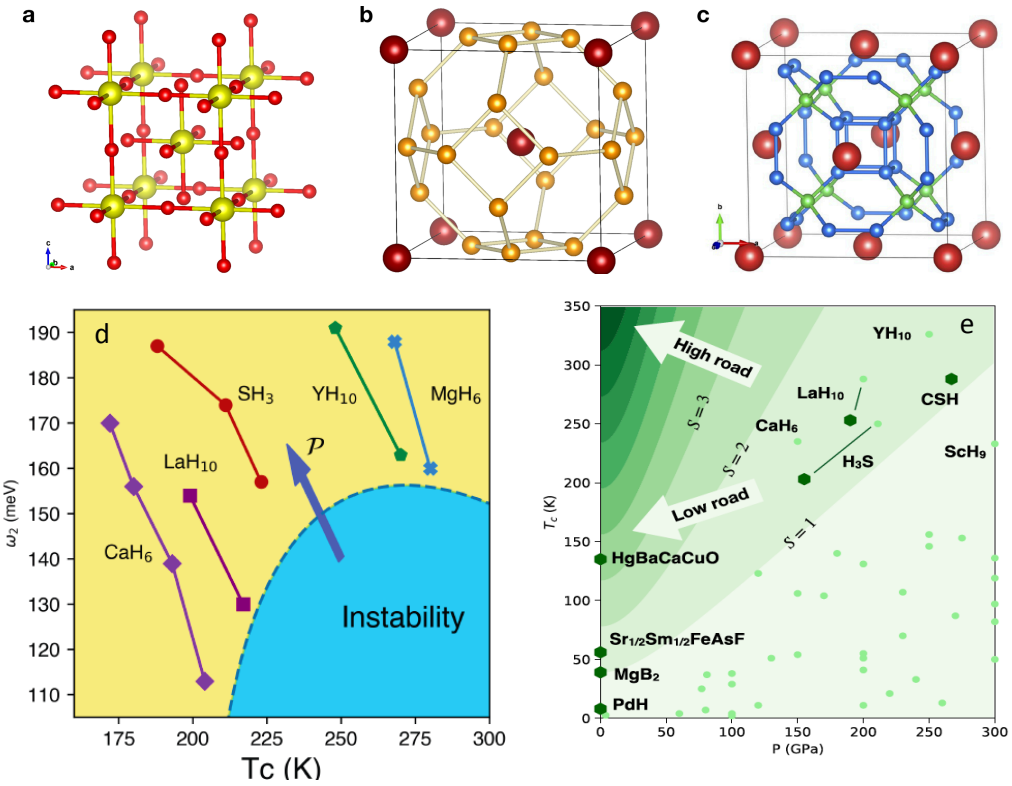

FIG. 3: (a-c). The structures of SH_3, YH_6, and LaH_{10}, respectively, illustrating the high symmetry and the progressions toward sodalite or clathrate-type structures with increased H content. (d) A schematic ω_2-T_c phase diagram of calculated results for five compressed hydrides in three crystal structure classes. Note that pressure is increasing in the upper left direction, blue denotes the low pressure region of instability of the structures that are considered. Pressure lowers T_c; as pressure increases, ω_2 increases but λ and T_c decrease. (e) Pickard's scatterplot in the P-T_c plane of experimental (hexagons) and theoretical (circles) positions for several superconductors. The contours indicate values of the *ad hoc* figure of merit $S = T_c(K)/[T_{c,MgB_2}(K)^2 + P(GPa)^2]^{1/2}$, which focuses attention on the desirability of low pressure P for higher T_c (see Ref. [[61], Sec. 12.]).

are coordinated only with two S atoms, see Fig. 3(a). Such a remarkably high prediction must have seemed to most readers as beyond comprehension, yet it was based on successful structure search algorithms and the established DFT-ME theory. Theoretical study of sulfur hydrides was confirmed and extended in 2015 by Akashi *et al.*[41] and Errea *et al.*,[42] which promoted the understanding of the relation of electronic structure and microscopic processes to promote high T_c.

Experiment. Independently, experimentalists were working on S-H samples. Even in 2014, Drozdov and collaborators[43] posted a notice of pressure-induced T_c=190K in sulfur hydride samples, and in 2015 the published announcement[44] was T_c as high as 203K around 160 GPa in the H-S system. The superconductor responded to magnetic field in the anticipated way, revealing the expected critical field $H_c(T)$ behavior versus temperature.

The sample was later determined by Einaga *et al.*[45] to have the bcc S sublattice predicted by Duan *et al.*, and it was concluded, based also on computational input, to be bcc SH_3 (denoted H_3S in the early literature) as shown in Fig. 3(a). The hydrogen→ deuterium isotope shift of T_c was large, as theory predicted, and T_c versus pressure was reproduced. This discovery opened the field to the possibility, indeed the likelihood, of room temperature superconductivity. High T_c in the T-P regime has been confirmed, for example by Huang *et al.* who reported from susceptibility measurements T_c as high as 183K around 150 GPa.[46]

C. LaH_{10}: approaching room temperature

Theory. The remarkable success of design and discovery for SH_3 emboldened the superconducting materials design community. Binary hydrides $\mathcal{M}H_n$ were the focus. Varying the metal $\mathcal{M}$ atom – valence, size, chemistry – and moving toward superhydrides ($n > 6$, say), would seem to approach the optimal combination toward the idealistic case of metallic hydrogen.

In 2017 two theoretical groups, Liu *et al.*,[47,48] and Peng *et al.*,[49] nearly simultaneously predicted $\mathcal{M}H_{10}$, with isovalent $\mathcal{M}$=La and Y, to have high T_c, in the 275-325K range depending on element and pressure (always above 200 GPa). Liu *et al.* calculated $\lambda = 2.2$, with T_c around 265K. The structure again was the highest symmetry possible for this stoichiometry, cubic with a clathrate-like shell of 32 H atoms surrounding the metal atom on its fcc sublattice, pictured in Fig. 3(c). Values for λ were in the 2.2-2.6 range, similar to SH_3 but also similar to Pb-Bi-Tl alloys from the 1970s with maximum T_c=9K that is 35 times lower.[18] The differences in T_c are due to the very high H vibrational frequencies (Ashcroft's primary point) while retaining strong coupling to Fermi surface electrons. Further studies of this superconductivity were provided by Liu *et al.*[50] and the quantum (zero point motion) nature of the structure by Errea *et al.*[51] Theoretical work by Ge *et al.*[52] indicates that doping LaH_{10} by B or N at the few percent level can raise T_c by 30K, *i.e.* to $T_c \approx$290K, in the 240 GPa regime.

Experiment. The superconducting materials discovery (experimental) community was also stimulated by the developments on SH_3. Synthesis and evidence of superconductivity in lanthanum superhydride around 260K was announced in two publications[53,54] in 2018-2019. Resistivity drops occurred in the 180-200 GPa range for various runs upon cooling and heating, and xray diffraction established the fcc sublattice of La, as in the LaH_{10} structural prediction. Superconductivity was confirmed by Drozdov and collaborators, initially at 215K [55] but soon thereafter up to 250K.[56]. The latter paper reported vanishing resistivity around 170 GPa, a H isotope effect, T_c decreasing with applied magnetic field, and evidence of the predicted crystal structure.

D. Yttrium superhydrides: the third discovery

Theory. The Y-H system has a more extensive history than S-H or La-H systems, partly because some of the design of La-H materials included the isovalent Y-H system. Li *et al.* reported[57] materials design for this system soon after their 2014 work on SH_2 noted in Sec. V.B. Their 2015 structure search at high pressure identified YH_3, a bct YH_4 lattice with both atomic H sites and H_2 units, and bcc YH_6 with a sodalite structure, [Fig. 3(b), Y surrounded by 24 H atoms] as promising candidates. The latter two had predicted T_c around 90K and 260K, respectively, in the (encouragingly low) 120 GPa pressure range.

The YH_6 prediction was startling on two counts: predicted T_c was 30% above the already remarkable SH_3 value of the previous year, and the required pressure was substantially lower. YH_6 contains some very strongly coupled H modes at comparatively low frequency (not far from instability), accounting for $\lambda \approx 3$ and high T_c in spite of (in fact, related to) the significantly lowered phonon energy scale ω_{log} (the logarithmic mean frequency[18]). However, anharmonicity and non-linear EP coupling can change predictions, especially when there are nearly unstable modes. These stoichiometries have not been reported in experimental studies as of 2022 (see below).

Peng *et al.* proposed[58] a focus on hydrogen clathrate structures as a route to RTS. Results for $\mathcal{M}H_n$ structures with $\mathcal{M}$=Y and La, for n=6, 9, 10, and $\mathcal{M}$=Sc for n=6 and 9 were presented. The results pertinent for this discussion are for two yttrium hydrides. YH_9 at 150 GPa has the largest calculated coupling: $\lambda \approx 4$, $T_c \approx$250K. However, YH_9 at 400 GPa has an even larger predicted T_c: $T_c \approx$290-300K with a smaller $\lambda \approx 2.3$. Considering the differences in structures and in optimum pressures, even their substantial amount of data only begins to provide guidelines for just what factors are most important in promoting RTS.

In 2019 Heil *et al.* predicted[59] clathrate-like structures from their structural search, focusing on YH_6 and YH_{10}. The results for YH_6 were similar to those of Li *et al.*[57], with calculated anharmonic effects accounting for some of the differences. T_c was predicted to be similar, 275K, for YH_6 at 100 GPa, an encouraging result for the efforts to produce and retain high T_c hydrides at more accessible pressures. For YH_{10} predicted T_c=300K around 300 GPa was obtained, similar to the results of Peng *et al.*[58]

For this compound a remarkably large coupling $\lambda \approx 4.5$ was reported, reproducing reasonably well results of Peng *et al.*[58] This value is perhaps the largest value from DFT-ME theory for a real (if still only predicted) compound. This large value of λ 'benefits' from very soft phonons, that is, being very close to a dynamical instability, which is a typical occurrence in several crystal classes.[60] When this occurs, corrections for anharmonicity, quantum fluctuations of H, and nonlinear EP coupling become necessary to pin down the critical pressure for instability as well as for the most complete prediction of T_c. Generally but especially in hydrides, low frequency modes do not promote T_c as much as their contribution to λ would suggest[60,61] (see Sec. VI.B).

Experiment. The experimental verification of the prediction of high T_c in the yttrium hydride YH_9 was announced[62] in 2019, and published in 2021: Kong *et al.*[63], T_c=243K at 200 GPa in space group $P6_3/mmc$, with the expected structure being clathrate-like. The compound YH_{10} predicted to have higher T_c was not observed in their experiments, which covered certain regions of phase space up to 410 GPa and 2250K. Snider *et al.*

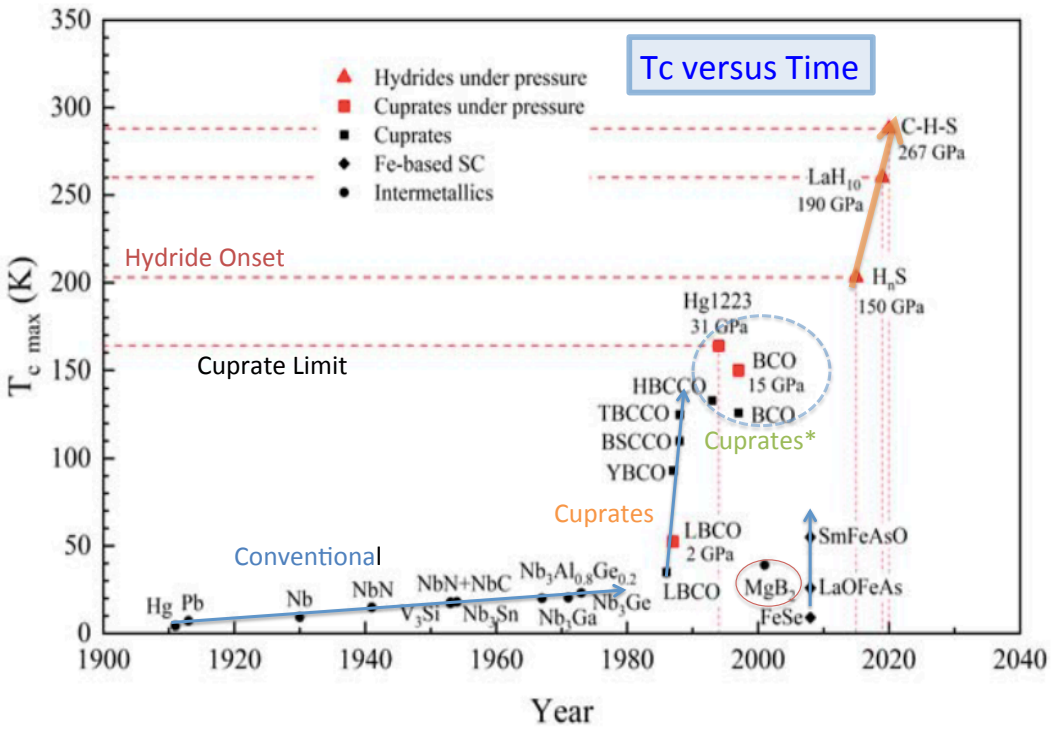

FIG. 4: A plot, from the beginning in 1911 and using linear scales, of the major advances in the maximum T_c versus year. Advances within classes are denoted by blue arrows. High pressure hydrides lie at the upper right, with temperatures converging on room temperature.

in 2021 provided data[64] indicating T_c up to 262 K for a sample with superconducting phase of stoichiometry likely close to YH_9 based on Raman data. This maximum T_c occurred around 180 GPa. Extension and some degree of confirmation was provided when T_c=253K was obtained in (La,Y)H_n mixtures by Semenok *et al.*[65]

As mentioned, other regions of the Y-H phase diagram have been predicted to display high temperature superconductivity. In 2021 Troyan *et al.* reported[66] T_c up to 224K at 166 GPa in cubic $Im\bar{3}m$ YH_6. This compound is an example of strong effects of anharmonicity (due to the structure and small proton mass). The calculated values are λ=2.4 using harmonic quantities, reduced to $\lambda = 1.7$ with anharmonic corrections. Anharmonicity considerably hardens the lower frequency H phonons, giving a calculated value of ω_{log}=115 meV and T_c in the range 180-230K depending on some choices. Nonlinear coupling corrections may be important to obtain the best predictions. Items to be award of when comparing predictions with data have been noted in Sec. V.A.

VI. CURRENT CHALLENGES

A. Further theoretical guidance

The progress in raising T_c over eleven decades of time is illustrated in Fig. 4. The lesson of the past was that increases in T_c cannot be foretold. On the other hand, the discovery of new superconductors with T_c approaching room temperature in compressed hydrides has been enabled by material-specific theory and computational materials design – near room temperature superconductivity was predicted, then verified by experiment. Intense effort continues toward discovering higher temperature or more accessible superconductors. The way forward appears optimistic, with some understanding of the microscopic processes being partnered by computational power in the search. In spite of the full DFT-ME theory that can be dug into at any level of detail that one wishes, helpful understanding may be slow to emerge.

In the previous section, some of the calculated values of EP coupling strength λ for the verified hydrides have been mentioned. The sample is small, but it has already been clear that λ in itself is a poor indicator

of T_c; increasing λ should not be the primary goal. Indications from Allen-Dynes analysis[18] through more recent studies[60] indicate that increasing the electron-proton scattering matrix element should become the focus of attention. Practically nothing is understood at present about what keeps I^2 large in the RTS materials when the electron gas is being compressed to higher density, and (in the simplest picture) should be screening more strongly, and reducing I^2. $N(0)$ itself is usually normal in size, which may help to promote stability. Several groups have noted that the H-atom DOS $N_H(0)$ per unit volume is likely to be the relevant quantity, but does not correlate strongly with T_c.

With leadership in materials design by the theoretical and computational modeling community, and materials discovery by high pressure experimenters with increasingly advanced techniques, the six decade old hope for room temperature has essentially been achieved: T_c up to the 250-260K range has been reproduced and accepted, at least partly due to agreement with prediction. The hurdle for closer study and application is that 150-300 GPa pressure is required. This observation directly suggests the two current primary goals: (1) yet higher T_c at high pressure, and ultimately superconducting atomic hydrogen, for the advancement of scientific achievement and for knowledge base, and (2) producing or retaining HTS to much lower, or preferably even ambient, pressure, for applications. The following comments provide items that could lead to advancement toward these goals. Some progress in these areas are noted in following subsections.

B. Analysis of H coupling

Analysis of strong EP coupling strength, especially at high frequency, is crucial in understanding how to increase T_c, since it contributes to both the frequency scale and to λ, and also helps to avoid structural instability. However, accomplishing this in compounds is more involved and less transparent than in elements because the relevant quantities – $N(0)$ (and $N_H(0)$), matrix elements, masses, and phonon frequencies – are mixtures of the constituent atoms and their interplay. Hydrides are special, besides their high T_c, because the large difference in the metal mass and the proton mass separates the phonon spectrum $F(\omega)$ and hence the Eliashberg spectral function $\alpha^2F(\omega)$ into separate frequency ranges:[60] low frequency metal acoustic modes separated by a gap from high frequency H optic modes. This separation is shown for the spectral function of SH_3 in Fig. 5. The separation of the degree of participation is almost complete. Whereas it has been common to quote the separate metal and H contributions to λ, as quoted for a few examples above, the capability of separating all of the atomic information is available from α^2F. This deeper analysis is important because λ alone is a poor indicator of T_c (see Sec. VI.B). What is of interest is the contribution to T_c (versus λ alone) from each atom. This analysis has been carried out for five hydrides in three crystal structures,[60] with some aspects arising in the following discussion.

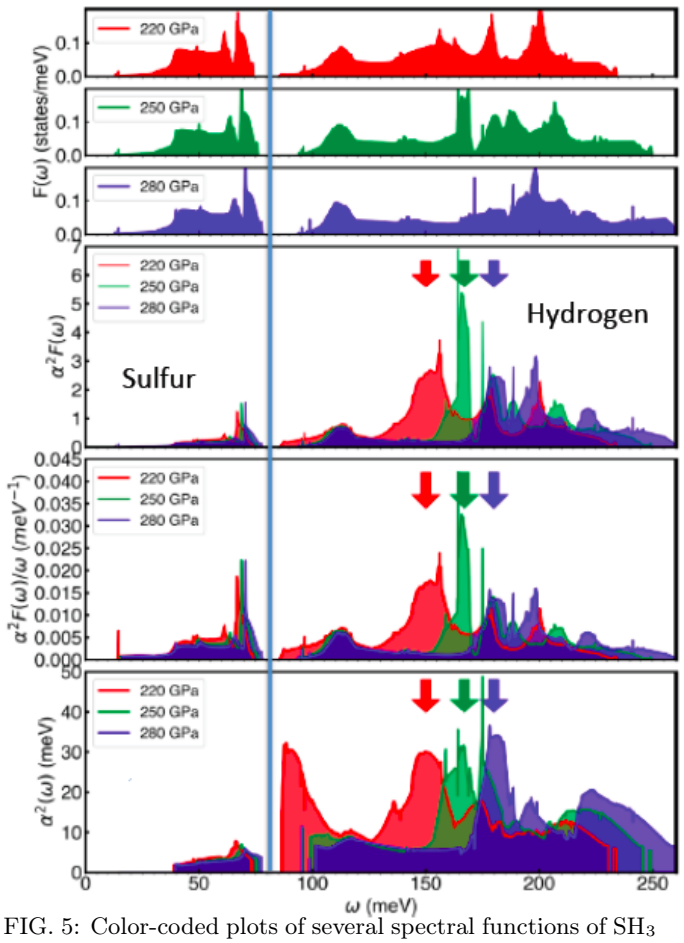

FIG. 5: Color-coded plots of several spectral functions of SH_3 at three pressures, all above the optimum pressure of 160K. The main point is to illustrate the separation of S and H modes, allowing analysis separately of their coupling strengths and contribution to T_c. The blue vertical line marks this separation, lying in the gap around 80 meV between S (left, low frequency) and H (right, high frequency) vibrational modes. Top three panels: phonon density of states $F(\omega)$ for each of the three pressures denoted. The main effect of pressure is to push some H modes to higher frequency. The bottom three panels show, respectively, $\alpha^2F(\omega)$, $\alpha^2F(\omega)/\omega$, and the ratio $\alpha^2(\omega)$=α^F/F that indicates the mean coupling matrix elements at frequency ω. The arrows indicates peaks of interest. The low frequency region is subject to numerical noise and has little weight so it has been cut out. Adapted with permission from Quan, Ghosh, and Pickett.[60]

1. *The metal-induced atomic hydrogen paradigm*

A leading paradigm in compressed hydrides is the need to break, or deter, the strong H_2 molecular bond, leaving open $1s$ shell atomic hydrogen rather than molecular hydrogen, which with no states at E_F is inert for EP coupling. Analysis based on the frequency separation of

metal and H modes was reported by Quan *et al.*[60] for five binary hydrides from three crystal structure classes. A phase diagram illustrating some aspects of the analysis is shown in Fig. 3(d). For brevity, only two of the main results will be mentioned.

First, although it is an appreciable fraction, the metal atom contribution to α^2F affects T_c very little, and sometimes lowers it, in which case the metal atom coupling is detrimental to T_c. This is possible because coupling to low frequency vibrations lowers the phonon frequency scale – the prefactor in T_c in Eqs. 1, 3, and 8 – negating the increase in λ. Quan *et al.* explain why this does not violate the Bergmann-Rainer 'theorem': additional coupling at one frequency affects the phonon spectrum and coupling at other frequencies. The net effect of the metal atom is very small and sometimes negative. This result focuses attention on H alone, providing a means for transparent understanding by neglecting the metal atom contribution.

Second, and following from the first: it is possible to extract and analyze the matrix element I_h^2 factor in Eq. 6 for scattering electrons from the moving H atom, as all other quantities in this equation are available. Quan *et al.* provide a discussion of this and several other aspects of EP coupling, arguing that understanding of I_H^2 is the main missing link in the understanding of EP coupling. A synopsis of some of their analysis is shown in Fig. 6. In the (η_H, λ_H) phase plane of Fig. 6(a) and the pressure dependencies of η_H, I_h^2 in Fig. 6(e), (f), respectively, the example hydrides seem to self-organize into groups. In the (κ_H, λ_H) plane and the other two pressure dependencies, the magnitudes and pressure behaviors of the five phases show considerable overlap. Note that in all cases I^2 increases with pressure, but (for example) the magnitudes at 300 GPa differ by a factor of 1.5.

As mentioned earlier, the strong tendency for I^2 to increase with pressure is counterintuitive, since the increased electronic density under volume reduction would seem to provide increased screening of H motion, thus reducing $I^2 = |<dV/dR_H>|^2$ (the average being over the Fermi surface). The increase indicates there is more physics to be understood. There is a simple and efficient approximation from Gaspari-Györffy (GG) theory, which uses a rigid potential displacement model. The result requires negligible computation, but involves phase shifts of the potential that do not provide a simple understanding. The GG model was applied to SH_3 by Papaconstantopoulos *et al.*[67], finding that η_H^{GG} rises steeply and nearly linearly from 18 $eV^2/Å^2$ at 200 GPa to 25 $eV^2/Å^2$ at 300 GPa. Fig. 6(f) indicates the extracted value (without approximation) of I_H^2 is 10-11 $eV^2/Å^2$ around 200 GPa, indicating a 70% overestimate by GG theory, with its neglect of screening. The calculations of Quan *et al.* were not extended to higher pressure, so a more complete comparison is not available. Hutcheon *et al.* have used GG theory to give a quick estimate of η in their machine learning study.[38].

2. *An alternative paradigm: activating bonding states*

The RTS examples introduced in Sec. V are from the anticipated class, in which hydrogen becomes atomic (no overt covalent bonding) and predominantly H 1*s* bands lie at the Fermi level and are primarily, almost overwhelmingly, responsible for high T_c. Computational explorations of ternary hydrides (see below) have found that at too low pressures, cells with molecular H_2 or H-rich molecules provide the stable structures. In such compounds, bonding and antibonding H 1*s* levels are split away from the Fermi level (below and above, respectively) and H vibrations provide little or no EP coupling. It seems that a guiding principle is that atomic H dominance leads over other productive possibilities, and its coupling strength requires further attention. Yet another possibility has arisen.

Gao *et al.* in 2021 reported a designed (predicted) H-rich system[68] in which high T_c (though not RTS) arises in a distinctive manner. The material is one in which BH_4 units (identifiable molecules) lie in interstitial positions within a bcc potassium sublattice, comprising $KB_2H_8 = K(BH_4)_2$. Extrapolating from results from other ternaries, such a compound should be unpromising. However, the chemistry (more specifically, the Madelung potential) is such that each molecular BH_4 radical (likely unstable in itself, lacking the extra electron that stabilizes methane CH_4) obtains $\frac{1}{2}$ electron from the K ion, leaving the uppermost (least strongly bound) molecular orbital half-empty. The resulting radicals are stable within the sublattice of positive K ions, and the compound is predicted to be dynamically stable.

KB_2H_8 is metallic, but with the character of a heavily hole-doped wide-gap insulator. This leaves covalently bonded bands that are strongly coupled to B-H bond-stretch modes at the Fermi level, a close analog[69] of MgB_2 with its T_c=40K. The calculation of Gao *et al.* gave T_c ≈140K, from very large λ=3 but an unusually low frequency scale ω_{log}=33 meV (100 meV is more typical of RTS hydrides). This is a three dimensional extension of the argument that such MgB_2-like systems can be optimized to produce much higher EP-coupled superconductivity.[70] Further improvements in this direction seem possible.

However, with such a large hole density that covalent bonds may be unstable, LiB_2H_8 may not be a thermodynamically stable composition. This scenario played out in $Li_{1-x}BC$, where for $x \sim 0.2 - 0.3$, T_c up to 75 K was calculated.[71] Substantial experimental effort[72] could not produce the desired structure at the target doping levels, obtaining instead distorted and disordered materials. However, Sr^{2+} doping on the K^{1+} sites, lowering the hole doping level, and broader synthesis routes may provide pathways to desired materials.[73]

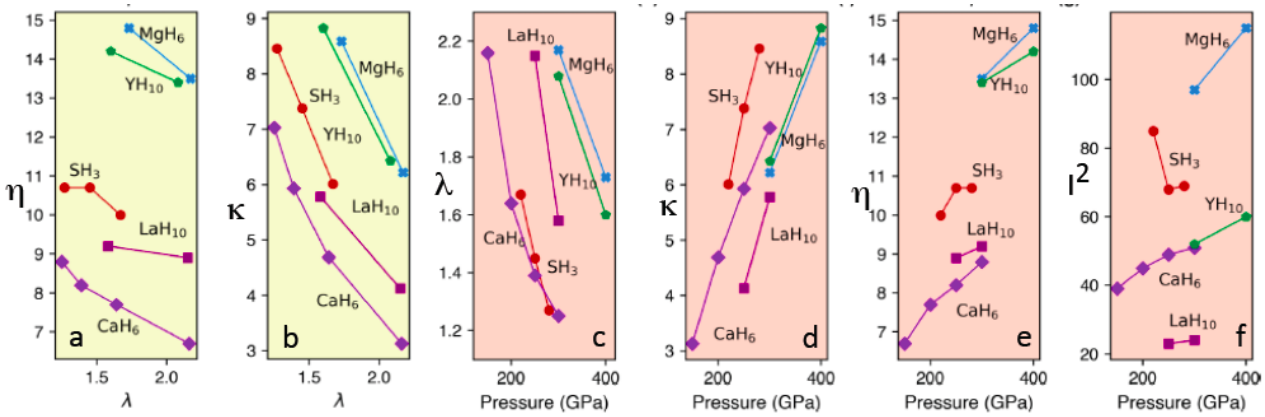

FIG. 6: Atomic H quantities in the indicated superconducting compressed hydrides, obtained by taking advantage of the spectral separation of metal acoustic modes and H optic modes. Corresponding calculated values of T_c can be seen in Fig. 3(d). (a,b) (η, λ) and (κ, λ) phase planes, respectively, indicating small (resp. large) relative variations. (c-f) Pressure variations of the indicated quantities, showing the magnitudes and rates of variation with pressure. Units: λ, unitless; $\eta = N(0)I^2$ and $\kappa = M_H\omega_2^2$, eV/Å^2; I^2, eV^2/Å^2. Adapted with permission from Quan, Ghosh, and Pickett.[60]

C. Increasing accessibility; retaining structures

Lowering the required pressure. Of growing concern is to find, perhaps by design and discover or perhaps by serendipity, materials that will display or retain the high values of T_c to lower pressures, with the intention of finding applications. (Refer to the preceding section.) Most of the binary hydrides have been explored with computational means.[74,75] Analysis of the results remains to be done, and unfortunately published results do not provide much of the information that is required, including the atom-specific quantities in λ in Eq. 6. The study of Quan *et al.* has initiated such analysis,[60] but was limited to a few binary hydrides for which their recalculations provided the data required for the analysis of the electronic properties.

Separately but equally valuable is an improved understanding of the stability, or lack thereof, of high T_c materials structures. Considering broadly, there are several examples of this scenario: a high T_c material is discovered (either computationally or experimentally) and its structure understood; pressure is lowered and T_c (and calculated λ) increases but a phonon branch is lowered; a structural phase transition occurs at a critical pressure P_{cr}; in the low pressure phase T_c is much lower or perhaps vanishing; the structure of the new phase includes H-rich molecular units, including possibly H_2, without much or any atomic hydrogen. One question being addressed is: how can this process be pushed to lower P_{cr}, or even (ideally) to ambient pressure.

More complex hydrides; speeding searches. After the design and discovery reported in the subsections above, emphasis has broadened. Higher values of T_c are of course still of great interest; after all, applications at room temperature will require T_c around 30% higher (375-400K). Given the considerable number of binary hydrides that have been modeled and mined for high T_c (here meaning roughly, T_c>100K), useful for applications), searches are being extended to ternary hydrides.

The palette of ternary hydrides is much larger than that of binaries, thereby opening new candidates. So far the emphasis has been on the more H-rich possibilities, viz. $A_iB_jH_n$ with small i and j and larger n. With atoms A and B selected from the (say) 60 most reasonable choices of elements, and with n ranging up to 12, this class has of the order of 10^4-10^5 formulae, and for each of these, many crystal structures are possible. Given this complexity, techniques in high-throughput computing, data set construction, data mining, coupled with machine learning, are being applied to the search for promising candidates, but a full search is not in sight. Some background on these activities can be found in the *2021 Roadmap* compilation.[61] There are too many reports already on ternary hydrides to attempt to provide an overview. Several candidates have predicted T_c >100K, however the explorations of the generalized convex hull to find the most stable stoichiometries have been limited.

Exploring higher pressures. While discussion of advancing high-pressure techniques is well beyond the scope of this article, it should be mentioned that experimental extensions to achieve higher pressures more readily, and to adapt measurement techniques to obtain more general data on the samples, are continually pursued in the high pressure laboratories that have contributed to high T_c hydrides at high pressure.

VII. REGULARITIES IN COMPRESSED HYDRIDES

While this article is not intended as a topical review of compressed hydrides, it should have raised questions

about the properties that provide close approach to room temperature superconductivity. Several features that appear to be important clues, *i.e.* to have some generality, have been identified.

• The overriding question is: what enables room temperature superconductivity? It is not large λ *per se*; $\lambda \approx$2-3 is similar to that in Pb alloys, with $T_c \approx$10K, with very soft phonons. Compressed hydrides have frequency scales up to 150-200 meV. The enabling feature is, as Ashcroft foretold, producing H-derived modes at high frequency while retaining strong coupling to Fermi surface carriers. This is, unfortunately, more an observation than an answer.

• Strong coupling. Barring innovations, larger(r) λ should not be the overriding aspiration. There are numerous cases, including compressed hydrides (see below), where increasing λ increases T_c but rapidly encounters soft phonons and lattice instability. λ is a poor descriptor for a high T_c search. Clue: η, independent of frequencies, is much better.[18,60] Since higher frequency scales will likely require ever higher pressures, the alternative seems to be pushing strong coupling to the high frequency region, which typically are the bond stretch modes.

• Various groups[76,77] have observed that atoms in columns I, II, and III provide, with occasional exceptions, the binary hydrides with high T_c. These atoms have low electronegativity, readily donating electrons to the H sublattice(s). The resulting negatively charged H atoms (versus neutral, half filled entities) promote breaking of H bonds and producing metallic ground states. This factor might also be related to the retention of strong coupling to high energy vibrations.

• Is a higher concentration of H the key? The indications are that a large fraction of H states at the Fermi surface, *i.e.* reflected in either large $N(0)$ or a large ratio $N_H/N(0)$, is not a clear determining factor, or at least is not essential. This is a straightforward band structure quantity, and cannot be estimated before the band calculation is done, because band structure effects cause structure in $N(\varepsilon)$. An example for this item: SH_3 is somewhat exceptional, with a strong van Hove peak at the Fermi level.[78] Pickard *et al.*[79] and Flores-Livas *et al.*[75] have highlighted the $N(0)$ factor in compressed hydrides.

• Producing atomic hydrogen, as opposed to molecular-bonded hydrogen, has been the overriding objective. Pressure will eventually decompose hydrogen molecules, but other methods (viz. doping) should be kept in mind. Doping holes into bonding states may be promising,[68] but too much doping will make the material prone to structural instabilities.

• Lattice instabilities. In several cases of high T_c hydrides, it has been found that within a given phase T_c decreases with increasing pressure. Conversely, T_c increases as pressure is decreased, λ increases, and the modes giving the increase in λ are renormalized to lower frequency and then become dynamically unstable. For the five systems illustrating this self-limiting process in Fig. 3(d), there is an indication of a phase boundary for binary hydrides in the ω_2-T_c plane.

• Naturally, the lattice stiffness $M_H\omega_{2,H}^2$ increases with pressure. However, strong coupling is far from uniform throughout the H-derived optic modes. Pressure does increase the frequency scale, but at the same time it decreases λ. This trade-off has long been a persistent issue when pursuing higher T_c superconductivity.

• The scattering efficacy of the vibrating H atom, I^2, increases with pressure.[60,67] The origin of this simple fact is unclear, but the theoretical and computational means to understand it is available within DFT codes (but requiring proper extraction).

• For the small set of examples that has been studied, I^2 varies from one to another over the pressure range of interest, by a factor of five, and η by a factor of two,[60] see Fig. 6. Again, the origin is unclear but the detailed computational theory exists to analyze this fact in detail.

• A separate type of question is: what structure types of compressed hydrides are favored, and in what pressure ranges? Some guidelines seem to have arisen. In the lower pressure range, hydrogen molecule phases dominate, and are poor superconductors or, often not reported, insulators. At higher pressure (say, 150-300 GPa, atomic hydrogen structures are frequently favored, with H-caged metal structures (*e.g.* clathrate) being common. At still higher pressures (with fewer published examples) less common structures are predicted; for example, one has several layers of hydrogen followed by a few layers of metal, suggestive of incipient phase separation. This area is a complex one, and the reviews and overviews mentioned below should be consulted.

A careful study of the "regularities" listed above will reveal apparent inconsistencies and contradictions. Example: strong coupling at high frequency is what is really important, but also $\eta = N(0)I^2$ (which is independent of frequency) is what really matters at strong coupling. Such various viewpoints are what must be confronted in the quest for higher T_c at lower pressure.

VIII. EPILOGUE

A number of overviews[79–82] and more extensive collections[36,61,74–76,83,84] on predictions of hydride superconductivity are available. The achievement of RTS has also stimulated extension of high pressure techniques and the enabling of additional measurements, in step with improved analysis and interpretation of data.[85,86]

The first point of this perspective was provided in Secs. II and III, which summarizes the sequence of theoretical and algorithmic advances, followed by numerical implementation, that have produced an accurate, material-specific theory of superconducting T_c as well as

several superconducting properties not discussed here, mostly stemming from the complex superconducting gap $\Delta(\omega, T)$. The three initial advances predicted by the theory and then confirmed by experiment are discussed in Sec. V:

- SH_3, 200K at 100 GPa
- LaH_{10}, 260K at 200 GPa
- YH_9, 240-260K around 250 GPa.

This article has been intended to provide an overview of the theory-driven forces behind the design and discovery of room temperature superconductivity. Room temperature superconductivity was a much discussed but distant goal in the 1970s, but expectations faded again after six years of cuprate HTS discoveries. The discovery of high T_c cuprates revived the dream to some extent, but it soon reverted to an intense study of the properties and mechanism of superconducting quantum materials that remains as a leading paradigm that is being broadened to other properties and applications. In terms of temperature, HTS has been superseded by compressed hydrides – the long-sought room temperature superconductors.

IX. ACKNOWLEDGMENTS

This overview has benefited from discussions with numerous colleagues over the past few years. This perspective was stimulated by communications with R. E. Cohen and R. J. Hemley, who confirmed my view that the impact of theory and materials design on searches for room temperature superconductivity should be chronicled. I acknowledge Yundi Quan and Soham Ghosh for collaboration on this topic in recent years.

[1] B. T. Matthias, Higher Temperatures and Instabilities, AIP Conf. Proc. **4**, 367 (1972); https://doi.org/10.1063/1.2946199.

[2] •1994 The Road to Room Temperature Superconductivity, Bodega Bay 1992.
•2005 Room Temperature Superconductivity. Notre Dame.
•2014 (Toward) Room Temperature Superconductivity, Leiden.
•2016 SUPERHYDRIDES Towards Room Temperature Superconductivity: Hydrides and More, Rome.
•2017 Towards Room Temperature Superconductivity: Superhydrides and More.
•2022 Challenges in designing Room Temperature Superconductors. L'Aquila, Italy.

[3] J. Bardeen, L. N. Cooper, and J. R. Schrieffer, Theory of Superconductivity, Phys. Rev. **108**, 1175 (1957).

[4] L. P. Gor'kov, On the energy spectrum of superconductors, Zh. Eksperim. i Teor. Fiz. **34**, 735 (1958); Sov. Phys. JETP **7**, 505 (1958).

[5] V. L. Ginzburg and L. D. Landau, On the theory of superconductivity, Zh. Eksp. Teor. Fiz. **20**, 1064 (1950).

[6] A. B. Migdal, Interactions between electrons and lattice vibrations in a normal metal, Sov. Phys. JETP **34**, 1438 (1960).

[7] G. M. Eliashberg, Temperature Green's function for electrons in a superconductor, Zh. Eksperim. i Teor. Fiz. **38**, 966 (1960); Sov. Phys. JETP **1**, 696 (1960).

[8] G. M. Eliashberg, Temperature Green's Functions for Electrons in a Superconductor, Zh. Eksperim. i Teor. Fiz. **38**, 1437 (1960); Sov. Phys. JETP **12**, 1000 (1961).

[9] P. Hohenberg and W. Kohn, Inhomogeneous Electron Gas, Phys. Rev. **140**, 864B (1964).

[10] W. Kohn and L. J. Sham, Self-Consistent Equations Including Exchange and Correlation, Phys. Rev. **140**, 1133A (1965).

[11] M. Lüders, M. A. L. Marques, N. N. Lathiotakis, J. A. Flores-Livas, G. Profeta, L. Fast, A. Continenza, S. Massidda, and E. K. U. Gross, Ab initio theory of superconductivity. I. Density functional formalism and approximate functionals, Phys. Rev. B **72**, 024545 (2005).

[12] D. J. Scalapino, J. R. Schrieffer, and J. W. Wilkins, Strong-Coupling Superconductivity I, Phys. Rev. **148**, 263 (1966).

[13] D. J. Scalapino, The Electron-Phonon Interaction and Strong-coupling Superconductivity, in *Superconductivity*, ed. R. D. Parks, (Marcel Dekker, Inc., New York, 1969), p. 561.

[14] W. L. McMillan, Transition Temperature of Strong-coupled Superconductors, Phys. Rev. **167**, 331 (1967).

[15] G. Bergmann and D. Rainer, The sensitivity of the transition temperature to changes in $\alpha^2F(\omega)$, Z. Phys. **263**, 59 (1973).

[16] P. B. Allen, Repulsive effect of low frequency phonons on superconductivity, Solid State Commun. **12**, 379 (1973) [Erratum Solid State Commun. **13**, *vii* (1973)].

[17] P. B. Allen, Effect of Soft Phonons on Superconductivity: a Re-evaluation ad a Positive Case for Nb_3Sn, Solid State Commun. **14**, 937 (1974).

[18] P. B. Allen and R. C. Dynes, Transition temperature of strong-coupled superconductors reanalyzed, Phys. Rev. B **12**, 905 (1975).

[19] P. B. Allen, Theory of Superconducting Transition Temperature, Pair Susceptibility, and Coherence Length, *Lecture Notes in Physics*, XVI Karpacz Winter School of Theoretical Physics (Springer-Verlag, 1979).

[20] P. B. Allen, Phonons and the Superconducting Transition Temperature, in *Dynamical Properties of Solids*, edited by G. K. Horton and A. A. Maradudin (North Holland, Amsterdam (?), 19xx).

[21] P. B. Allen and B. Mitrović, Theory of Superconducting T_c, in *Solid State Physics* **37**, ed. H. Ehrenreich, F. Seitz, and D. Turnbull (Academic, New York, 1982).

[22] N. W. Ashcroft, Metallic Hydrogen: a High-Temperature Superconductor? Phys. Rev. Lett. **21**, 1748 (1968).

[23] J. M, McMahon and D. Ceperley, High-Temperature Superconductivity in Atomic Metallic Hydrogen, Phys. Rev. B **84**, 144515 (2011).

[24] N. W. Ashcroft, Hydrogen dominant metallic alloys: high temperature superconductors? Phys. Rev. Lett. **92**, 187002 (2004).

[25] A. A. Mostofia, J. R. Yates, Y.-S. Lee, I. Souza, D. Van-

derbilt, and N.Marzari, wannier90: A tool for obtaining maximally-localised Wannier functions, Comp. Phys. Commun. **178**, 685 (2008).
[26] K. M. Rabe and U. V. Wagmare, Localized basis for effective lattice Hamiltonians: Lattice Wannier functions, Phys. Rev. B **52**, 13236 (1995).
[27] E. Cockayne, Generation of lattice Wannier functions via maximum localization, Phys. Rev. B **71**, 094302 (2005).
[28] F. Giustino, Electron-phonon interactions from first principles, Rev. Mod. Phys. **89**, 015003 (2017).
[29] F. Giustino, *Materials Modeling using Density Functional Theory: Properties and Predictions* (Oxford University Press, Oxford, 2014).
[30] Y. Yang, J. Lv, L. Zhu, and Y. Ma, CALYPSO: A method for crystal structure prediction, Comp. Phys. Comm. **183**, 2063 (2012).
[31] C. W. Glass, A. R. Oganov, and N. Hansen, USPEX – evolutionary crystal structure prediction, Comp. Phys. Comm. **175**, 713-720 (2006).
[32] C. J. Pickard and R. J. Needs, Ab initio random structure searching, J. Phys.:Condens. Matt. **23**, 053201 (2011).
[33] D. C. Lonie and E. Zurek, XtalOpt: an open-source evolutionary algorithm for crystal structure prediction, Phys. Commun. **181**, 372 (2011).
[34] See Ref. [36] for references.
[35] *Modern Methods of Crystal Structure Prediction*, ed. A. R. Oganov (Wiley-VCH, Berlin, 2010). ISBN 978-3-527-40939-6.
[36] K. P. Hilleke and E. Zurek, Tuning Chemical Precompression: Theoretical design and crystal chemistry of novel hydrides in the quest for warm and light superconductivity at ambient pressures, J. Appl. Phys. **131**, 070901 (2022).
[37] D. Duan, X. Huang, F. Tian, D. Li, H. Yu, Y. Liu, Y. Ma, B. Liu, and T. Cui, Pressure-induced decomposition of solid hydrogen sulfide, Phys. Rev. B **91**, 180502 (2015).
[38] M. J. Hutcheon, A. M. Shipley, and R. J. Needs, Predicting novel superconducting hydrides using machine learning approaches, Phys. Rev. B **101**, 144505 (2020).

$\rightarrow\rightarrow$ SH_3 references

[39] Y. Li, J. Hao, H. Liu, Y. Li, and Y. Ma, The metalization and superconductivity of dense hydrogen sulfide, J. Chem. Phys. **140**, 174712 (2014).
[40] D. Duan, Y. Liu, F. Tian, D. Li, X. Huang, Z. Zhao, H. Yu, B. Liu, W. Tian, and T. Cui, Pressure-induced metalization of dense $(H_2S)_2H_2$ with high-T_c superconductivity. Sci. Rep. **4**, 6968 (2014).
[41] R. Akashi, M. Kawamura, S. Tsuneyuki, Y. Nomura, and R. Arita, First-principles study of the pressure and crystal structure dependences of the superconducting transition temperature of compressed sulfur hydrides, Phys. Rev. B **91**, 060511(R) (2015).
[42] I. Errea, M. Calandra, C. J. Pickard, J. Nelson, R. J. Needs, Y. Li, H. Liu, Y. Zhang, Y. Ma, and F. Mauri, High-Pressure Hydrogen Sulfide from First Principles: A Strongly Anharmonic Phonon-Mediated Superconductor, Phys. Rev. Lett. **114**, 157004 (2015).
[43] A. P. Drozdov, M. I. Eremets, and I. A. Troyan, Conventional superconductivity at 190K at high pressures, arXiv:1412.0460.
[44] A. P. Drozdov, M. I. Eremets, I. A. Troyan, V. Ksenofontov, and S. I. Shylin, Conventional superconductivity at 203 kelvin at high pressures in the sulphur hydride system, Nature (London) **525**, 73 (2015).
[45] M. Einaga, M. Sakata, T. Ishikawa, K. Shimizu, M. Eremets, A. Drozdov, I. Troyan, N. Hirao, and Y. Ohishi, Crystal Structure of 200 K-Superconducting Phase of Sulfur Hydride System, Nat. Phys. **12**, 835 (2016).
[46] X. Huang, X. Wang, D. Duan, B. Sundqvist, X. Li, Y. Huang, H. Yu, F. Li, Q. Zhou, B. Liu, and T. Cui, Natl. Sci. Rev. **6**, 713 (2019).

$\rightarrow\rightarrow$ LaH_{10} references

[47] H. Liu, I. I. Naumov, R. Hoffman, N. W. Ashcroft, and R. J. Hemley, Potential high T_c superconducting lanthanum and yttrium hydrides at high pressure, Proc. Natl. Acad. Sci. **114**, 6990 (2017). https://doi.org/10.1073/pnas.1704505114
[48] H. Liu, I. I. Naumov, Z. M. Geballe, m. Somayazulu, J. S. Tse, and R. J. Hemley, Dynamics and superconductivity in compressed lanthanum superhydride, Phys. Rev. B **98**, 100102(R) (2018).
[49] F. Peng, Y. Sun, C. J. Pickard, R. J. Needs, Q. Wu, and Y. Ma, Hydrogen Clathrate Structures in Rare Earth Hydrides at High Pressures: Possible Route to Room-Temperature Superconductivity, Phys. Rev. Lett. **119**, 107001 (2017).
[50] L. Liu, C. Wang, S. Yi, K. W. Kim, J. Kim, and J.-H. Cho, Origin of High-Temperature Superconductivity in Compressed LaH_{10}, Phys. Rev. B **99**, 140501 (2019).
[51] I. Errea, F. Belli, L. Monacelli, A. Sanna, T. Koretsune, T. Tadano, R. Bianco, M. Calandra, R. Arita, F. Mauri, and J. A. Flores-Livas, Quantum crystal structure in the 250-kelvin superconducting lanthanum hydride, Nature **578**, 66 (2020). arXiv:1907.11916.
[52] Y. Ge, F. Zhang, and R. J. Hemley, Room-temperature superconductivity in boron- and nitrogen-doped lanthanum superhydride, Phys. Rev. B **104**, 214505 (2021).
[53] Z. M. Geballe, H. Liu, A. K. Mishra, M. Ahart, M. Somayazulu,Y. Meng, M. Baldini,R. J. Hemley, Synthesis and Stability of Lanthanum Superhydrides, Angew. Chem. Intl. Ed. **57**, 688 (2018).
[54] M. Somayazulu, M. Ahart, A. K. Mishra, Z. M. Geballe, M. Baldini, Y. Meng, V. V. Struzhkin, and R. J. Hemley, Evidence for superconductivity above 260 K in lanthanum superhydride at megabar pressures, Phys. Rev. Lett. **122** 027001 (2019); arXiv:1808.07695.
[55] A. P. Drozdov, V. S. Minkov, S. P. Besedin, M. A. Kuzovnikov, D. A. Knyazev, and M. I. Eremets, Superconductivity at 215 K in lanthanum hydride at high pressures, arXiv: 1808.07039.
[56] A. P. Drozdov, P. P. Kong, V. S. Minkov, S. P. Besedin, M. A. Kuzovnikov, S. Mozaffari, L. Balicas, F. F. Balakirev, D. E. Graf, V. B. Prakapenka, E. Greenberg, D. A. Knyazev, M. Tkacz and M. I. Eremets, Superconductivity at 250 K in lanthanum hydride under high pressures, Nature **569**, 528 (2019). arXiv:1812.01561

$\rightarrow\rightarrow$ YH_n references

[57] Y. Li, J. Hao, H. Liu, J. S. Tse, Y. Wang and Y. Ma, Pressure-stabilized superconductive yttrium hydrides, Sci. Rep. **5**, 9948 (2015).
[58] F. Peng, Y. Sun, C. J. Pickard, R. J. Needs, Q. Wu, and Y. Ma, Hydrogen Clathrate Structures in Rare Earth Hydrides at High Pressures: Possible Route to Room-Temperature Superconductivity, Phys. Rev. Lett. **119**,

107001 (2017).
[59] C. Heil, S. di Cataldo, G. B. Bachelet, and L. Boeri, Superconductivity in sodalite-like yttrium hydride clathrates, Phys. Rev. B **99**, 220502 (2019).
[60] Y. Quan, S. S. Ghosh, and W. E. Pickett, Compressed hydrides as metallic hydrogen superconductors, Phys. Rev. B **100**, 184505 (2019).
[61] The 2021 Room-Temperature Superconductivity Roadmap, L. Boeri *et al.*, J. Phys.: Condens. Matter **32**, (2021). doi: 10.1088/1361-648X/ac2864
[62] P. P. Kong, V. S. Minkov, M. A. Kuzovnikov, S. P. Besedin, A. P. Drozdov, S. Mozaffari, L. Balicas, F. F. Balakirev, V. B. Prakapenka, E. Greenberg, D. A. Knyazev, and M. I. Eremets, Superconductivity up to 243 K in yttrium hydrides under high pressure, arXiv:1909.10482.
[63] P. P. Kong, V. S. Minkov, M. A. Kuzovnikov, A. P. Drozdov, S. P. Besedin, S. Mozaffari, L. Balicas, F. F. Balakirev, V. B. Prakapenka, S. Chariton, D. A. Knyazev, E. Greenberg, and M. I. Eremets, Superconductivity up to 243 K in the yttrium-hydrogen system under high pressure, Nature Commun. **12**, 5075 (2021).
[64] E. Snider, N. Dasenbrock-Gammon, R. McBride, X. Wang, N. Meyers, K. V. Lawler, E. Zurek, A. Salamat, and R. P. Dias, Synthesis of Yttrium Superhydride Superconductor with a Transition Temperature up to 262K by Catalytic Hydrogenation at High Pressures, Phys. Rev. Lett. **126**, 117003 (2021).
[65] D. V. Semenok, I. A. Troyan, A. G. Kvashnin, A. G. Ivanova, M. Hanfland, A. V. Sadakov, O. A. Sobolevskiy, K. S. Pervakov, A. G. Gavriliuk, I. S. Lyubutin, K. V. Glazyrin, N. Giordano, D. N. Karimov, A. B. Vasiliev, R. Akashi, V. M. Pudalov, and A. R. Oganov, Superconductivity at 253 K in lanthanum-yttrium ternary hydrides, Mater. Today **48**, 18 (2021).
[66] I. A. Troyan, D. V. Semenok, A. G. Kvashnin, A. V. Sadakov, O. A. Sobolevskiy, V. M. Pudalov, A. G. Ivanova, V. B. Prakapenka, E. Greenberg, A. G. Gavriliuk, I. S. Lyubutin, V. V. Struzhkin, A. Bergara, I. Errea, R. Bianco, M. Calandra, F. Mauri, L. Monacelli, R. Akashi, A. R. Oganov, Anomalous High-Temperature Superconductivity in YH_6, Adv. Mater. **33**, 2006832 (2021).

→→ C-S-H references

[67] D. A. Papaconstantopoulos, B. M. Klein, M. J. Mehl, and W. E. Pickett, Cubic H3S around 200 GPa: An atomic hydrogen superconductor stabilized by sulfur, Phys. Rev. B **91**, 184511 (2015).
[68] M. Gao, X.-W. Yan, Z.-Y. Lu, and T. Xiang, Phonon-mediated high-temperature superconductivity in the ternary borocarbide KB_2H_8 under pressure near 12 GPa, Phys. Rev. B **104**, L100504 (2021).
[69] J. M. An and W. E. Pickett, Superconductivity of MgB_2: Covalent Bonds Driven Metallic, Phys. Rev. Lett. **86**, 4366 (2001).
[70] W. E. Pickett, The Next Breakthrough in Phonon-Mediated Superconductivity, Physica C **468**, 126-135 (2008).
[71] H. Rosner, A. Kitaigorodsky, and W. E. Pickett, Prediction of High T_c Superconductivity in Hole-doped LiBC, Phys. Rev. Lett. **88**, 127001 (2002).
[72] A. M. Fogg, J. B. Claridge, G. R. Darling, and M. J. Rosseinsky, Synthesis and Characterization of Li_xBC —- Hole Doping Does Not Induce Superconductivity, Chem. Commun. **9**, 1348 (2003).
[73] Y.Nakamori and S.-I. Orimo, Synthesis and Characterization of Single Phase Li_xBC (x = 0.5 and 1.0), Using Li Hydride as a Starting Material, J. Alloys & Compounds **370**,
[74] T. Bi, N. Zarifi, T. Terpstra, and E. Zurek, The Search for Superconductivity in High Pressure Hydrides, in *Elsevier Reference Module in Chemistry, Molecular Sciences and Chemical Engineering*, edited by J. Reedijk (Elsevier, Waltham, MA, 2017). arXiv:1806.00163.
[75] J. A. Flores-Livas, L. Boeri, A. Sanna, G. Profeta, R. Arita, and M. Eremets, A perspective on conventional high-temperature superconductors at high pressure: Methods and materials, Phys. Rep. **856**, 1 (2020). arXiv:1905.06693
[76] D. V. Semenok, I. A. Kruglov, I. A. Savkin, A. G. Kvanhnin, and A. R. Oganov, On Distribution of Superconductivity in Metal Hydrides, Current Opinion in Solid State and Materials Science **24**, 100808 (2020).
[77] F. Belli, T. Novoa, J. Contreras-Garcia, and Y. Errea, Strong correlation between electron bonding network and critical temperature in hydrogen-based superconductors, Nat. Commun. **12**, 5381 (2021].
[78] S. S. Ghosh, Y. Quan, and W. E. Pickett, Strong particle-hole asymmetry in a 200 Kelvin superconductor, Phys. Rev. B **100**, 094521 (2019). -
[79] C. J. Pickard, I. Errea, and M. I. Eremets, Superconducting Hydrides Under Pressure, Ann. Rev. Condens. Matt. Phys. **11**, 57 (2020). arXiv:1910.00385

→→ Final references

[80] W. E. Pickett and M. Eremets, The Quest for Room-Temperature Superconductivity in Hydrides, Physics Today **72**, 51-57 (2019).
[81] L. Boeri and G. B. Bachelet, Viewpoint: the road to room-temperature conventional superconductivity, J. Phys.: Condens. Matt. **31**, 234002 (2019).
[82] K. Shimizu, Investigation of Superconductivity in Hydrogen-rich Systems, J. Phys. Soc. Jpn. **89**, 051005 (2020).
[83] E. Zurek and T. Bi, High Temperature Superconductivity in Alkaline and Rare Earth Polyhydrides at High Pressures: A Theoretical Perspective, (2019). arXiv:1810.12338
[84] K. P. Hilleke, T. Bi, and E. Zurek, Materials under high pressure: A chemical perspective, arXiv:2112.15193
[85] R. J. Hemley, M. Ahart, H. Liu, and M. Somayazulu, Road to Room-Temperature Superconductivity: Tc above 260 K in Lanthanum Superhydride under Pressure, arXiv:1906.03462
[86] P.-W. Guan, R. J. Hemley, and V. Viswanathan, Combining pressure and electrochemistry to synthesize superhydrides, Proc. Natl. Acad. Sci. **118**, e2110470118 (2021); https://doi.org/10.1073/pnas.2110470118
[87] Y. Sun, J. Lv, Y. Xie, H. Liu, and Y. Ma, Route to a Superconducting Phase above Room Temperature in Electron-Doped Hydride Compounds under High Pressure, Phys. Rev. Lett. **123**, 097001 (2019).